β-Catenin Directs Long-Chain Fatty Acid Catabolism in the Osteoblasts of Male Mice

Julie L. Frey,[1] Soohyun P. Kim,[1] Zhu Li,[1] Michael J. Wolfgang,[2] and Ryan C. Riddle[1,3]

[1]Department of Orthopaedic Surgery, Johns Hopkins University School of Medicine, Baltimore, Maryland 21205; [2]Department of Biological Chemistry, Johns Hopkins University School of Medicine, Baltimore, Maryland 21205; and [3]Veterans Administration Medical Center, Baltimore, Maryland 21201

Wnt-initiated signaling through a frizzled receptor and the low-density lipoprotein–related receptor-5 coreceptor instructs key anabolic events during skeletal development, homeostasis, and repair. Recent studies indicate that Wnt signaling also regulates the intermediary metabolism of osteoblastic cells, inducing glucose consumption in osteoprogenitors and fatty acid utilization in mature osteoblasts. In this study, we examined the role of the canonical Wnt-signaling target, β-catenin, in the control of osteoblast metabolism. *In vitro*, Wnt ligands and agonists that stimulated β-catenin activation in osteoblasts enhanced fatty acid catabolism, whereas genetic ablation of β-catenin dramatically reduced oleate oxidation concomitant with reduced osteoblast maturation and increased glycolytic metabolism. Temporal ablation of β-catenin expression in osteoblasts *in vivo* produced the expected low-bone-mass phenotype and also led to an increase in white adipose tissue mass, dyslipidemia, and impaired insulin sensitivity. Because the expression levels of enzymatic mediators of fatty acid β-oxidation are reduced in the skeleton of β-catenin mutants, these results further confirm the role of the osteoblast in lipid metabolism and indicate that the influence of Wnt signaling on fatty acid utilization proceeds via its canonical signaling pathway. (***Endocrinology* 159: 272–284, 2018)**

Engagement of a frizzled receptor and the low-density lipoprotein–related receptor (Lrp) 5 or Lrp6 coreceptor by a Wnt ligand regulates the stability and nuclear translocation of β-catenin (1). Within the osteoblast lineage, signals that enhance the nuclear abundance of β-catenin are essential for normal bone mass accrual (2–5) and exert differentiation stage-specific effects on osteoblast function. During early bone development, β-catenin is required for the initial fate specification of osteoblasts as they differentiate from bipotential, osteochondroprogenitors (6–8). In committed osteoblasts, β-catenin regulates cellular proliferation (9, 10), facilitates the attainment of a mature phenotype (11–13), and regulates the expression of osteoprotegerin, a decoy receptor that opposes Rank ligand–stimulated osteoclast differentiation (11, 13, 14).

Recent studies indicate that Wnt signaling in the osteoblast is also instructive in the regulation of cellular metabolism. However, the specific role of β-catenin in this process remains unclear. In *in vitro* studies, Esen and colleagues (15) demonstrated that Wnt3a stimulates glucose consumption and glycolysis in osteoblastic cell lines, including ST2 cells that bear similarity to marrow stromal cells (16). Subsequent gene knockdown experiments revealed that this effect did not involve β-catenin but instead proceeded via the activation of Rac1, which in turn stimulated mammalian target of rapamycin (mTOR) complex 2-Akt signaling and posttranscriptional regulation of glycolytic enzyme expression. Similarly, Wnts have been reported to stimulate glutamine catabolism by activating mTOR signaling (17).

In our prior work (18), we demonstrated that Wnt signaling through the Lrp5 coreceptor enhances fatty acid oxidation by mature osteoblasts and that genetic overexpression of β-catenin in cultured osteoblasts increased oxidation potential. Mice lacking Lrp5, but not those

ISSN Online 1945-7170

Received 19 September 2017. Accepted 20 October 2017.
First Published Online 25 October 2017

Abbreviations: ATP, adenosine triphosphate; CTX, C-terminal telopeptide of type 1 collagen; GFP, green fluorescent protein; IP, intraperitoneal; Lrp, low-density lipoprotein–related receptor; mRNA, messenger RNA; mTOR, mammalian target of rapamycin; P1NP, procollagen type 1 amino-terminal propeptide; PCR, polymerase chain reaction; qPCR, quantitative polymerase chain reaction; RRID, Research Resource Identifier; TM, tamoxifen.

lacking the closely related Lrp6, specifically in osteoblasts and osteocytes, accumulate adipose tissue with reduced whole-body energy expenditure and increased levels of circulating lipids. Likewise, the specific ablation of the gene encoding Cpt2, an obligate enzyme in fatty acid catabolism, in osteoblasts impaired bone mass accrual and produced a dyslipidemia (19).

In these studies, we explored the effect of β-catenin loss of function on osteoblast metabolism. We report that Wnt ligands that stimulate β-catenin transcriptional activity in osteoblasts also stimulate fatty acid oxidation and that β-catenin is required for normal fatty acid metabolism in osteoblasts. Moreover, temporal ablation of β-catenin expression in mature osteoblasts *in vivo* results in an increase in adiposity with impairments in fatty acid and glucose metabolism as well as the expected loss of bone mass. Together, these data suggest that Wnt signaling directs fatty acid metabolism via a canonical mechanism involving the activation of β-catenin.

Methods

Animal models

The Institutional Animal Care and Use Committee of the Johns Hopkins University approved all procedures involving mice. Mice containing *loxP* sites in intron 1 and 6 of the *Ctnnb1* gene (20) were obtained from Jackson Laboratories (stock no. 004152) and crossed with Oc-CreER^{T2} mice (21) in which the expression of Cre-ER^{T2} is directed by the human osteocalcin promoter. Oc-CreER^{T2} mice were also crossed with ROSA$^{mT/mG}$ mice (Jackson Laboratories; stock no. 007676) to evaluate temporal control of gene recombination. Polymerase chain reaction (PCR) analysis of tail biopsy specimens was used to confirm genotypes and all mice were maintained on a C57BL/6 background. To induce gene recombination of floxed Ctnnb1 alleles or the ROSA locus, CreER^{T2}-positive mice and their CreER^{T2}-negative littermates were administered tamoxifen (TM), 150 ng/g body weight, by intraperitoneal (IP) injection on 5 consecutive days. Oc-CreER^{T2}; ROSA$^{mT/mG}$ mice were evaluated 3 days after the last TM injection, and Oc-CreER^{T2}; Ctnnb1$^{flox/flox}$ mice were evaluated 8 weeks after the last TM injection.

Culture of primary osteoblasts

Primary mouse osteoblasts were isolated from the calvaria of 1- to 3-day-old neonates by serial digestion in 1.8 mg of collagenase/mL. For *in vitro* deletion of β-catenin, cultures of osteoblasts isolated from Oc-CreER^{T2}; Ctnnb1$^{flox/flox}$ mice were treated with 1 μM TM for 2 days. Osteoblast differentiation was induced by supplementing α-minimal essential medium containing 10% serum with 10 mM β-glycerol phosphate and 50 μg ascorbic acid/ml. Differentiation was confirmed by alkaline phosphatase and Alizarin red S staining according to standard techniques. Wnt ligands (100 ng/mL; R&D Systems) and pharmacological agonists of Wnt signaling (10 μM; EMD Millipore) signaling were added 6 or 18 hours before analysis.

Gene expression studies

Total RNA was extracted from osteoblast cultures or mouse tissues using TRIzol (Life Technologies). For skeletal tissue, the femur was cleaned of soft tissue, the growth plate was removed, and the marrow cavity was flushed with phosphate-buffered saline. Reverse transcription reactions were carried out by using 1 μg of RNA and the iScript cDNA synthesis system (Bio-Rad). Real-time quantitative PCR (qPCR) was carried out by using iQ Sybr green Supermix (Bio-Rad) with primer sequences obtained from PrimerBank (Massachusetts General Hospital). Reactions were normalized to endogenous β-actin reference transcripts. Cellular protein was collected in Triton X-100 lysis buffer and prepared for immunoblotting according to standard technique. Antibodies specific for active β-catenin [unphosphorylated on Ser33/Ser37/Thr41; catalog no. 8814; Research Resource Identifier (RRID): AB_11127203], β-catenin (catalog no. 8480; RRID: AB_11127855), phosphorylated-Akt (Ser473; catalog no. 9271; RRID: AB_329825), and Akt (catalog no. 9272; RRID: AB_329827) for immunoblotting were obtained from Cell Signaling Technology.

In vitro metabolic studies

Fatty acid and glucose oxidation were measured in flasks with stoppers equipped with center wells, as previously described (22). Cultures were differentiated for 7 days before analysis and then incubated at 37°C in media containing 0.5 mM L-carnitine, 0.2% bovine serum albumin, and either ^{14}C-oleate (PerkinElmer) or ^{14}C-glucose. $^{14}CO_2$ was captured and counted by the addition of 1 N perchloric acid to the reaction mixture and 1 M NaOH to the center well containing Whatman filter paper. The acidified reaction mixture was incubated overnight at 4°C and centrifuged at 4000 rpm for 30 minutes before aliquots of the supernatant were counted for ^{14}C-labeled acid soluble metabolites. Glucose uptake was assessed by using 2-deoxy-D-[^{3}H]-glucose, as previously described (23). Lactate levels were assessed by using a Lactate assay kit (Sigma-Aldrich). Cellular adenosine triphosphate (ATP) levels were quantified via a bioluminescent assay (ATP bioluminescent assay HSII; Roche).

Skeletal phenotyping

High-resolution images of the mouse femur and L5 vertebra were acquired by using a desktop microtomographic imaging system (Skyscan 1172; Bruker) in accordance with the recommendations of the American Society for Bone and Mineral Research (24). Bones were scanned at 50 keV and 200 μA using a 0.5-mm aluminum filter with an isotropic voxel size of 10 μm. In the femur, trabecular bone parameters were assessed in the 500 μm proximal to the growth plate and extending for 2 mm (200 computed tomographic slices). In the spine, trabecular bone parameters were assessed between the cranial and caudal growth plates. The resulting two-dimensional cross-sectional images are shown in grayscale. Static and dynamic bone formation was assessed by injection of two sequential 0.25-mL doses of calcein (0.8 mg/mL) delivered 3 and 8 days before euthanasia. The spine was fixed in ethanol, dehydrated, and embedded in methylmethacrylate. Three-micron sections were cut with a microtome and stained with Mason-Goldner trichrome stain. The numbers of osteoblasts and osteoclasts per bone perimeter were measured at standardized sites in the L5 vertebrae at a magnification of ×200 using a semiautomatic method (Osteoplan II; Kontron). These parameters comply with the guidelines of the nomenclature committee of the American

Society for Bone and Mineral Research (25, 26). For histological examination of bone marrow adiposity, femurs were decalcified in 10% EDTA before being sectioned and stained with hematoxylin and eosin according to standard techniques. Serum analysis of collage deposition and degradation products procollagen type 1 amino-terminal propeptide (P1NP) and C-terminal telopeptide of type 1 collagen (CTX) was completed by using enzyme-linked immunosorbent assays from Immunodiagnostic Systems.

Metabolic studies and bioassays

Glucose levels were measured by using a OneTouch Ultra (LifeScan) hand-held glucose monitor. For glucose tolerance testing, glucose (1 g/kg body weight) was injected via the IP route after an overnight fast. For insulin tolerance testing, mice were fasted for 4 hours and then injected via the IP route with insulin (0.2 U/kg body weight). Plasma triglycerides (Sigma-Aldrich), β-hydroxybutyrate (Sigma-Aldrich), cholesterol (Bio-Assay Systems), free fatty acids (Sigma-Aldrich), and glycerol (Sigma-Aldrich) were measured colorimetrically in plasma collected from random fed mice collected 3 hours after the initiation of the light cycle. Plasma insulin (Alpco) and under-carboxylated osteocalcin (Takara) were assessed by enzyme-linked immunosorbent assay. Insulin signaling in white adipose tissue and liver was assessed by injection of insulin (0.5 U/kg) into the portal vein before tissue excision and snap freezing for immunoblot analysis (27, 28). Pancreata were fixed and stained with an anti-insulin antibody (DAKO; catalog no. A056401; RRID: AB_2617169), and islet morphometry was assessed as previously described (29). Sections of gonadal white adipose tissue and liver were stained with hematoxylin and eosin.

Statistics

All results are presented as mean ± standard error of the mean. Statistical analyses were performed by using unpaired, two-tailed Student's *t* or analysis of variance tests followed by *post hoc* tests. A P value <0.05 was considered to indicate a statistically significant difference. In all figures, the asterisk indicates $P \leq 0.05$.

Results

Canonical Wnt ligands enhance fatty acid oxidation by osteoblasts *in vitro*

Recent studies have detailed the expression patterns of Wnt ligands within developing and mature bone (9, 30, 31). As a first step in characterizing the mechanism by which Wnt signaling regulates fatty acid catabolism in the osteoblast, we examined the ability of Wnt ligands that are highly expressed in bone to increase the oxidation of fatty acids *in vitro*. Wnt2b, Wnt3a, Wnt10b, and Wnt16 stimulation of cultured osteoblasts for 18 hours induced canonical Wnt/β-catenin signaling, as indexed by increases in active, unphosphorylated β-catenin, total cellular β-catenin levels (Fig. 1A) and the expression levels of the β-catenin target gene Axin2 (Fig. 1B) (32, 33). In turn, these ligands induced a 15% to 25% increase in the oxidation of ^{14}C-labeled oleate to $^{14}CO_2$ (Fig. 1C) and significantly increased the messenger RNA (mRNA) levels of enzymatic mediators of fatty acid utilization (Fig. 1D). By contrast, oleate oxidation was unaffected by noncanonical ligands Wnt4, Wnt5a, Wnt5b, and Wnt11, which also had no effect on active or total β-catenin protein levels or the expression of Axin2. Indeed, the expression levels of Acadl, one of the enzymes that catalyzes the initial step in mitochondrial β-oxidation of straight-chain fatty acids, was significantly downregulated by Wnt4, Wnt5a, and Wnt5b treatment.

To confirm these studies, we also treated cultured osteoblasts with pharmacological agonists of Wnt/β-catenin signaling (Fig. 1E–1G). 2-Amino-4-(3,4-(methylenedioxy)benzylamino)-6-(3-methoxyphenyl) pyrimidine (also referred to as Wnt agonist) (34), and SKL2001, which antagonizes the interaction of Axin and β-catenin (35), increased the expression of Axin2, enhanced oleate oxidation, and mirrored the effects of canonical Wnt ligand stimulation on the mRNA levels of Acadl, Acads, Acadvl, and Cpt1b. These results suggest that the effects of Wnt signaling on fatty acid catabolism proceed via the stabilization and activation of β-catenin.

β-Catenin loss of function impairs osteoblast differentiation and fatty acid oxidation *in vitro*

β-Catenin is required for the initial fate specification of osteoblastic cells, and its genetic ablation in osteoprogenitors and osteoblasts results in the accumulation of chondrocytes and early lethality in mice (4, 6, 7, 11). To circumvent these phenotypes and directly examine the role of β-catenin in osteoblast metabolism *in vitro* and *in vivo*, we crossed Ctnnb1$^{flox/flox}$ mice (20) with Oc-CreER^{T2} mice (21) to generate mice and osteoblast cultures in which recombination of *Ctnnb1* could be temporally controlled.

The addition of TM to cultures of calvarial osteoblasts isolated from Ctnnb1$^{flox/flox}$ (control) and Oc-CreER^{T2}; Ctnnb1$^{flox/flox}$ (ΔCtnnb1) mice from days 5 to 7 of induction in osteogenic medium produced significant reductions in β-catenin mRNA levels and those of the Wnt-target genes Axin2 and Nkd2 in CreER^{T2}-positive osteoblasts (Fig. 2A). As expected, loss of β-catenin function was also associated with a marked impairment in osteoblast differentiation; both the expression of genes encoding runx2, osterix, osteocalcin, type I collagen, and osteoprotegerin and the mineralization of the extracellular matrix were significantly reduced (Fig. 2B and 2C).

To determine whether β-catenin regulates osteoblast metabolism, we examined the ability of control and ΔCtnnb1 cultures to oxidize ^{14}C-labeled substrates. Consistent with the notion that activation of β-catenin signaling favors fatty acid oxidation, the oxidation of oleate to CO_2 and acid soluble metabolites, products of incomplete oxidation, was reduced by 43% and 60%,

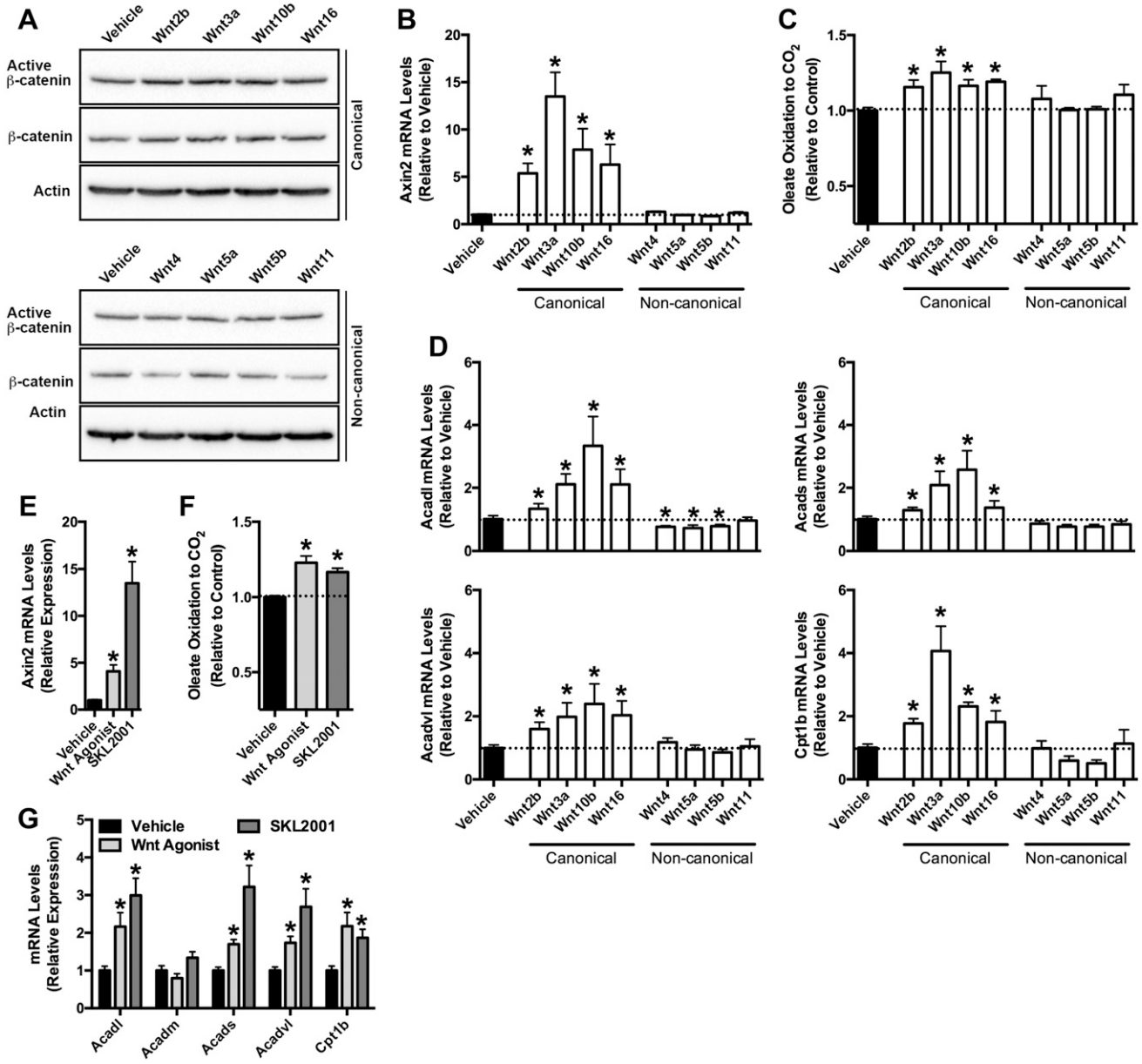

Figure 1. Canonical Wnts and Wnt agonists increase fatty acid oxidation in osteoblasts. (A) Immunoblot analysis of active β-catenin (unphosphorylated on Ser33/Ser37/Thr 41) and total β-catenin levels 18 hours after Wnt ligand (100 ng/mL) stimulation. (B) qPCR of Axin2 mRNA levels in primary osteoblasts stimulated with Wnt ligands for 18 hours. (C) Relative oxidation of ^{14}C-Oleate to $^{14}CO_2$ by osteoblasts treated with Wnt ligands for 18 hours. Results were normalized to protein concentration and then expressed relative to the untreated control. (D) qPCR analysis of Acadl, Acads, Acadvl, and Cpt1b mRNA levels in osteoblasts treated with Wnt ligands. (E) Axin2 mRNA levels in primary osteoblasts treated with Wnt agonist [2-amino-4-(3,4-(methylenedioxy)benzylamino)-6-(3-methoxyphenyl)pyrimidine, 10 μM] or SKL2001 (10 μM) for 18 hours. (F) Relative oxidation of ^{14}C-Oleate to $^{14}CO_2$ by osteoblasts treated with Wnt agonist or SKL2001. (G) qPCR analysis of genes involved in fatty acid catabolism in osteoblasts treated with Wnt agonist or SKL2001. All *in vitro* data were replicated in two independent studies. Data are expressed as mean ± standard error of the mean. $^*P < 0.05$.

respectively, in ΔCtnnb1 osteoblasts relative to controls (Fig. 2D and 2E). Likewise, the mRNA levels of genes involved in mitochondrial fatty acid β-oxidation were significantly downregulated by β-catenin loss of function (Fig. 2F). The reduced capacity of ΔCtnnb1 osteoblasts to oxidize fatty acid did not result in a compensatory increase in the oxidation of glucose (Fig. 2G). Instead, mutant osteoblasts exhibited a shift to glycolytic metabolism. Glucose uptake was increase by 37% (Fig. 2H) whereas lactate levels were increased by 88% (Fig. 2I) in ΔCtnnb1 osteoblasts relative to controls. Additionally, a subset of genes involved in glycolysis were upregulated in osteoblasts lacking β-catenin (Fig. 2J). However, the shift in substrate selection in ΔCtnnb1 osteoblasts was unable to maintain cellular ATP at levels similar to those in control osteoblasts (Fig. 2K), suggesting that the loss of β-catenin function and ensuing decrease in fatty acid oxidation result in an energy deficit.

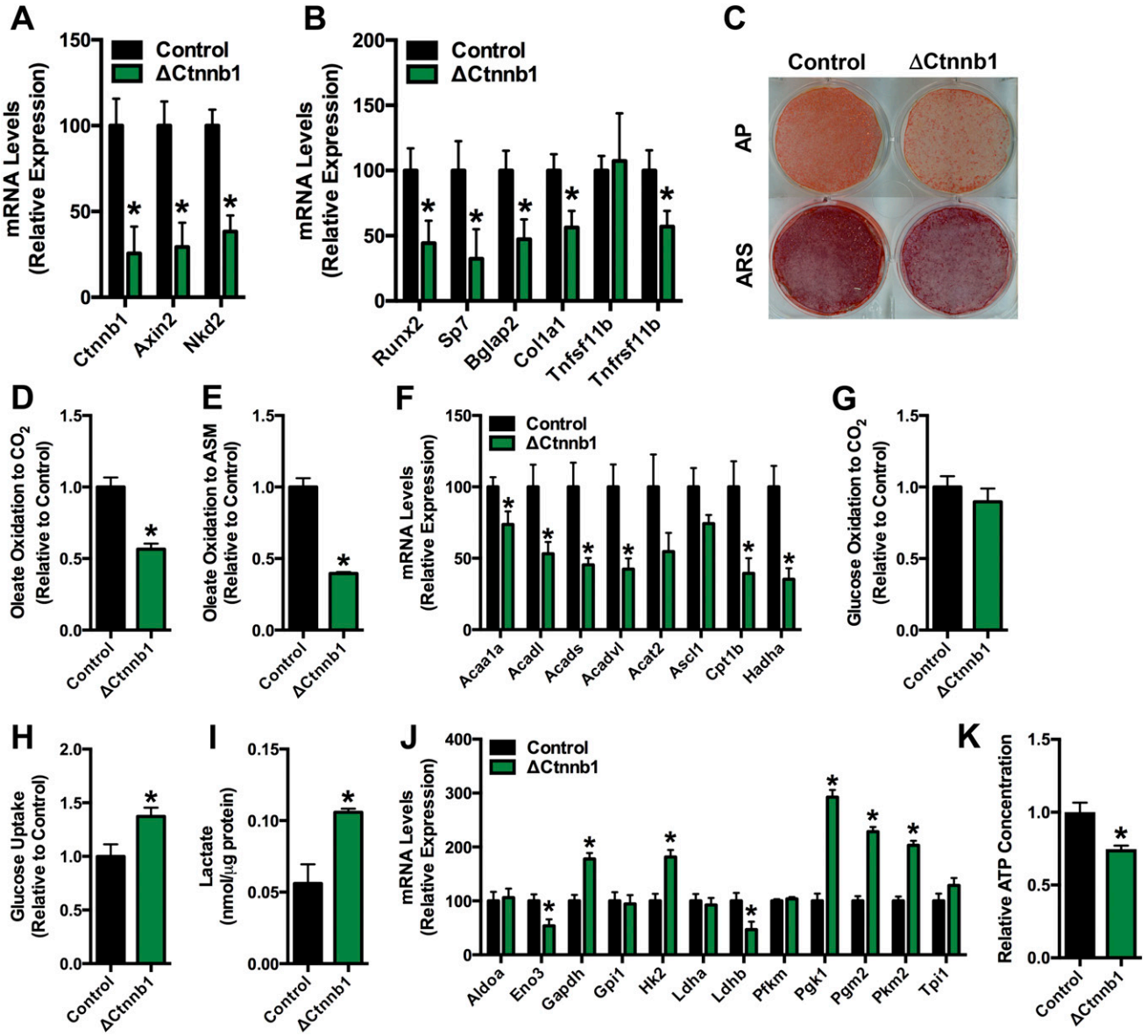

Figure 2. Fatty acid oxidation is reduced in osteoblasts lacking β-catenin. (A) qPCR analysis of Ctnnb1, Axin2, and Nkd2 mRNA levels in primary osteoblasts isolated from Ctnnb1$^{flox/flox}$ (Control) and Oc-CreER^{T2}; Ctnnb1$^{flox/flox}$ (ΔCtnnb1) mice treated with 1 μM tamoxifen on days 5 to 7 and then cultured in osteogenic medium for an additional 2 days. (B) qPCR analysis of markers of osteoblastic cells in control and ΔCtnnb1 osteoblasts. (C) Alkaline phosphatase (AP) and Alizarin red S (ARS) staining of cultures of control and ΔCtnnb1 osteoblasts cultured for an additional 7 days after TM administration as in (A). (D and E) Relative oxidation of ^{14}C-Oleate to (D) $^{14}CO_2$ and (E) acid-soluble metabolites (ASM) by control and ΔCtnnb1 osteoblasts. (F) qPCR analysis of genes involved in fatty acid catabolism by control and ΔCtnnb1 osteoblasts. (G) Relative oxidation of ^{14}C-glucose to $^{14}CO_2$. Results were normalized to protein concentration and then expressed relative to the control osteoblast cultures. (H) Relative uptake of 2-deoxy-D-[^{3}H]-glucose. (I) Cellular lactate levels in control and ΔCtnnb1 osteoblasts cultured in osteogenic media for 7 days. (J) qPCR analysis of genes involved in glucose catabolism in control and ΔCtnnb1 osteoblast cultures. (K) Cellular ATP levels in control and ΔCtnnb1 osteoblasts. Results were normalized to protein concentration and then expressed relative to the control osteoblast cultures. All *in vitro* data were replicated in two independent studies. Data are expressed as mean ± standard error of the mean. *$P < 0.05$.

Temporal ablation of β-catenin expression in the mature osteoblast leads to high bone turnover

We next sought to examine the effect of β-catenin loss of function on skeletal homeostasis and whole-body metabolism *in vivo*. However, to ensure that the level of gene deletion was sufficient and that recombination was limited to the osteoblast lineage, we first examined recombination in Oc-CreER^{T2}; ROSA$^{mT/mG}$ mice, wherein gene recombination leads to a shift from red fluorescent protein expression to green fluorescent protein (GFP) expression. Eight-week-old male mice were administered TM (150 ng/g body weight) or vehicle (sunflower seed oil) on 5 consecutive days, and tissue samples were collected at 9 weeks of age (Fig. 3A). No GFP expression was detected in the femurs of vehicle-treated mice (Fig. 3B and 3E) or CreER^{T2}-negative, ROSA$^{mT/mG}$ mice treated with TM (Fig. 3D). Gene recombination was detected in most presumptive osteoblasts lining bone

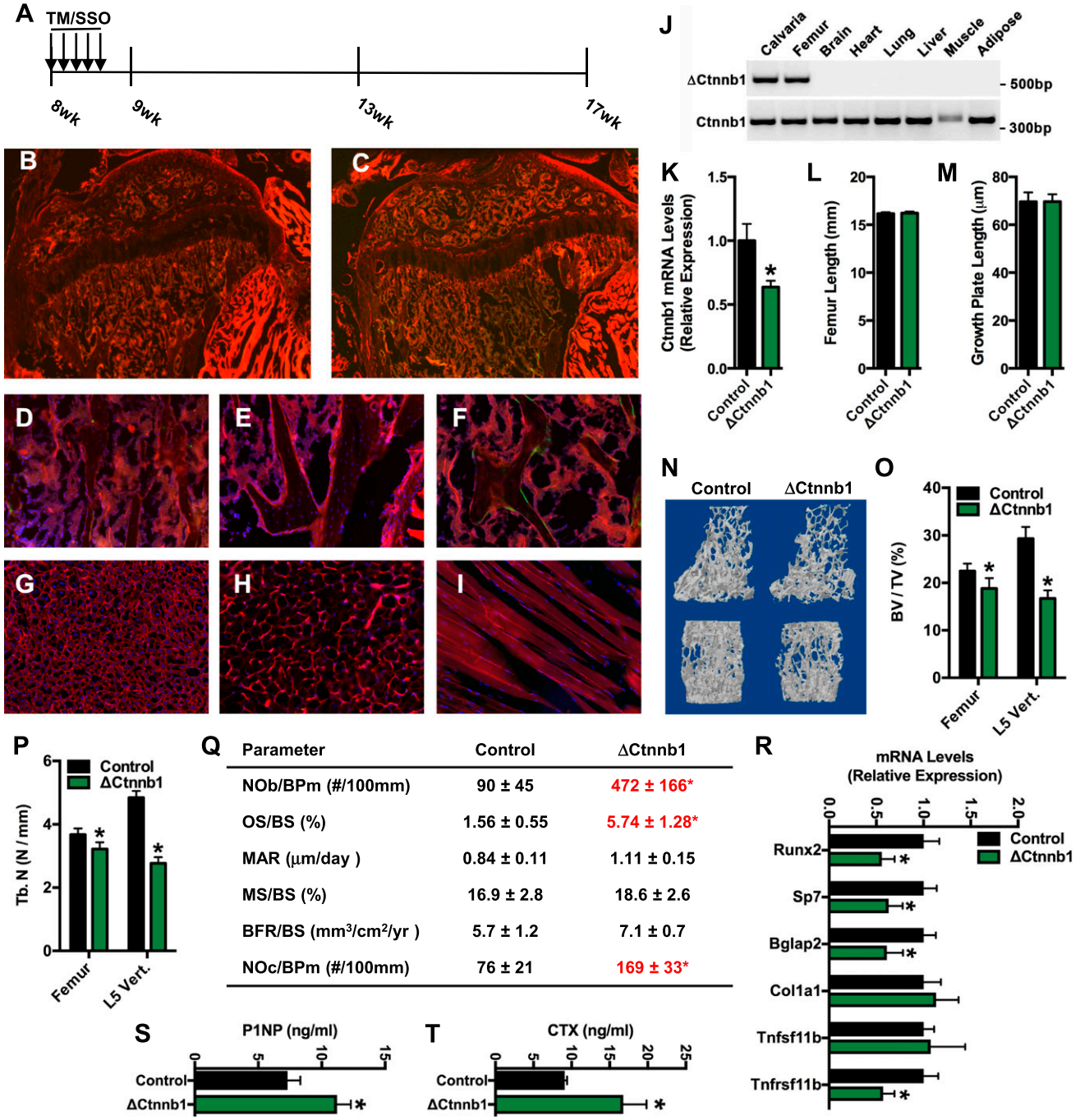

Figure 3. Temporal ablation of β-catenin expression reduces bone volume. (A) Schematic representation of experimental design. Eight-week-old mice were treated with TM (150 ng/g body weight) or sunflower seed oil (SSO) on 5 consecutive days and then euthanized at 9 weeks of age or at 17 weeks of age. (B and C) Immunofluorescent analysis of gene recombination in Oc-CreER^{T2}; ROSA$^{mT/mG}$ treated with (B) SSO or (C) TM at 9 weeks of age (Original magnification ×4). (D–F) Immunofluorescent analysis of gene recombination in the trabecular bone compartment of ROSA$^{mT/mG}$ mice treated with (D) TM, Oc-CreER^{T2}; ROSA$^{mT/mG}$ mice treated with (E) SSO, and Oc-CreER^{T2}; (F) ROSA$^{mT/mG}$ mice treated with TM. (G–I) Immunofluorescent analysis of gene recombination in the (G) liver, (H) gonadal fat pad, and (I) skeletal muscle of Oc-CreER^{T2}; ROSA$^{mT/mG}$ mice treated with TM. (J) Allele-specific PCR analysis of *Ctnnb1* gene recombination in tissue isolated from Oc-CreER^{T2}; Ctnnb1$^{flox/flox}$ mice (ΔCtnnb1) at 17 weeks of age (8 weeks after TM injection). (K) qPCR analysis of Ctnnb1 mRNA levels in the femur of control and ΔCtnnb1 mice. (L) Femur length and (M) growth plate length in control and ΔCtnnb1 mice at 17 weeks of age. (N) Representative computer renderings of trabecular bone structure in the distal femur (top) and L5 vertebrae (bottom) in control and ΔCtnnb1 mice. (O) Quantification of trabecular bone volume per tissue volume (BV/TV) in the distal femur and L5 vertebrae. (P) Quantification of trabecular bone number (Tb. N). (Q) Quantification of static and dynamic indices of bone turnover in 17-week-old control and ΔCtnnb1 mice. (R) qPCR analysis of phenotypic markers of osteoblastic cells in the femur of control and ΔCtnnb1 mice. (S and T) Serum levels of (S) P1NP and (T) CTX in control and ΔCtnnb1 mice. Data are expressed as mean ± standard error of the mean; n = 5 to 8 mice per group. *$P < 0.05$. BFR, bone formation rate; BPm, bone perimeter; BS, bone surface; MAR, mineral apposition rate; MS, mineralizing surface; NOb; osteoblast number; NOc, osteoclast number; OS, osteoid surface.

surfaces in both the primary and secondary ossification centers, but not in the growth plate, of TM-treated Oc-CreER^{T2}; ROSA$^{mT/mG}$ mice (Fig. 3C). Indeed, closer examination revealed that approximately 50% of the cuboidal osteoblasts lining trabecular bone surfaces were GFP positive (Fig. 3F). Importantly, no GFP expression was detected in extraskeletal tissues, including the liver, gonadal fat pad, and skeletal muscle, of these mice (Fig. 3G–3I), indicating that Oc-CreER^{T2} is specific for osteoblastic cells.

We used the same TM treatment strategy to disrupt the expression of *Ctnnb1* in osteoblasts in Oc-CreER^{T2}; Ctnnb1$^{flox/flox}$ (hereafter referred to as ΔCtnnb1) and maintained mice, as well as TM-treated Ctnnb1$^{flox/flox}$ (hereafter referred to as control) littermates for an additional 8 weeks. As in the ROSA$^{mT/mG}$ cross, TM-stimulated recombination was limited to skeletal tissue (Fig. 3J), and qPCR analyses of mRNA isolated from the femur revealed a nearly 40% reduction in the expression of β-catenin 8 weeks after TM treatment.

Postnatal disruption of β-catenin expression had no effect on longitudinal bone growth (Fig. 3L and 3M), but high-resolution micro–computed tomographic analysis demonstrated that the mutant mice developed the expected osteopenic phenotype (Fig. 3N). Trabecular bone volume per tissue volume was significantly reduced in the distal femur and to a greater extent in the L5 vertebrae of the mutant mice (Fig. 3O) and was secondary to reductions in trabecular bone number (Fig. 3P). Static and dynamic histomorphometric analyses performed on the L5 vertebrae suggested that low bone volume was due to the development of a state of high bone turnover (Fig. 3Q). Osteoblast numbers per bone perimeter were dramatically increased in ΔCtnnb1 mice relative to controls, but, consistent with our *in vitro* findings, these cells were functionally impaired as the osteoid surface per bone surface was more than 3.5-fold higher in mutants. Additionally, and in support of this interpretation, the mineral apposition rate and the mineralizing surface in ΔCtnnb1 mice were similar to those in control mice, despite the increase in the numbers of osteoblasts. The mRNA levels of osteoblastic markers were reduced in the femurs of the mutant mice (Fig. 3R), partially mirroring the effect of β-catenin disruption *in vitro*. In line with previous studies showing that β-catenin signaling in osteoblasts regulates osteoclast development (14), osteoclast numbers per bone perimeter were also markedly increased in ΔCtnnb1 mice. The development of a state of high bone turnover was further confirmed by serum analyses of the collagen deposition and degradation products P1NP and CTX, which were significantly increased in the mutant mice relative to controls (Fig. 3S and 3T). Therefore, temporal disruption of β-catenin in the mature osteoblast results in bone loss due to accelerated bone resorption and impaired osteoblastic bone formation.

β-Catenin mutants accumulate white adipose tissue

In accordance with the impaired capacity of cultured ΔCtnnb1 osteoblasts to oxidize fatty acids (Fig. 2D and 2E), qPCR analysis of samples isolated from the femurs of ΔCtnnb1 mice disclosed severe reductions in the expression of genes involved in fatty acid catabolism relative to control mice (Fig. 4A). We questioned whether these alterations in gene expression might in turn be associated with a change in body composition. In the 8 weeks following TM administration, the body weight of ΔCtnnb1 mice was similar to that of control littermates (Fig. 4B). However, at necropsy, the weights of major white adipose tissue depots were increased in the mutant mice relative to controls (Fig. 4C), whereas the weights of other major organs were unaffected (Fig. 4D).

Histological examination of tissues from ΔCtnnb1 mice indicated that the accumulation of white adipose tissue was due to adipocyte hypertrophy and accompanied by ectopic lipid deposition (Fig. 4E). Adipocyte size was significantly increased in the gonadal fat pad of mutants relative to controls (Fig. 4E and 4F) and qPCR analysis of gene expression in this tissue revealed a significant increase in the mRNA levels of genes associated with *de novo* fatty acid synthesis and triglyceride storage (Fig. 4G). The liver of ΔCtnnb1 mice exhibited a modest but consistent increase in the vacuolization of hepatocytes that is associated with lipid deposition (Fig. 4E). Indeed, liver triglycerides were significantly increased in ΔCtnnb1 mice relative to controls (Fig. 4H), despite reduced expression of key genes involved in lipid synthesis (*i.e.*, Acaca and Fasn) (Fig. 4I) and normal expression of catabolic genes (Fig. 4J). The abundance of marrow adipocytes was not affected by the loss of β-catenin function in mature osteoblasts and osteocytes (Fig. 4E and 4K).

β-Catenin mutants accumulate white adipose tissue and have impaired lipid and glucose metabolism

On the basis of our experience with mice lacking the Lrp5 coreceptor in osteoblasts (18), we suspected that the increased adiposity in ΔCtnnb1 mice might be accompanied by alterations in the serum lipid profile. Serum triglyceride, cholesterol, and ketone levels were similar in control and ΔCtnnb1 mice (Fig. 5A–5C), but free fatty acid levels were elevated in the mutant mice (Fig. 5D). This is unlikely to be due to an increase in lipolysis because serum glycerol levels were similar to those in controls (Fig. 5E) and adipose tissue maintained a gene expression profile compatible with increased lipid deposition (Fig. 4G). Rather, the increase in serum fatty

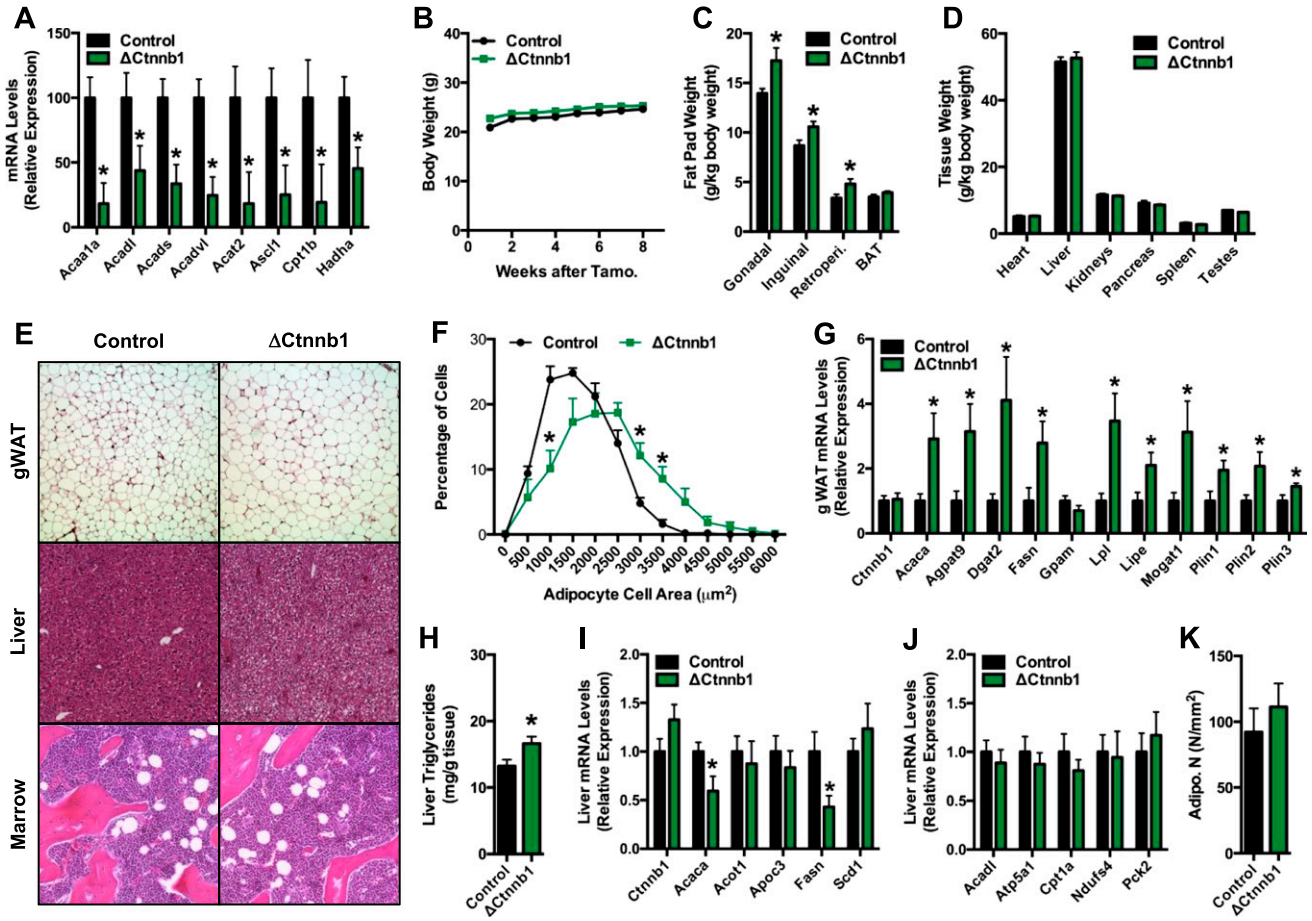

Figure 4. Fat mass is increased in ΔCtnnb1 mice. (A) qPCR analysis of genes involved in fatty acid catabolism in the femur of control and ΔCtnnb1 mice. (B) Body weight of control and ΔCtnnb1 mice. (C and D) Weights of (C) major fat pads and (D) organs in 17-week-old control and ΔCtnnb1 mice. (E) Representative hematoxylin and eosin–stained sections of gonadal white adipose tissue (gWAT), liver, and marrow of control and ΔCtnnb1 mice (original magnification ×10). (F) Quantification of adipocyte size in gWAT. (G) qPCR analysis of genes in fatty acid anabolism and storage in gWAT. (H) Quantification of triglycerides in liver biopsy specimens isolated from control and ΔCtnnb1 mice. (I and J) qPCR analysis of genes involved in (I) fatty acid anabolism and (J) catabolism in the liver of control and ΔCtnnb1 mice. (K) Quantification of adipocyte numbers in the trabecular bone compartment of the femur. Data are expressed as mean ± standard error of the mean; n = 5 to 9 mice per group. *$P < 0.05$. BAT, brown adipose tissue.

acids in mutant mice is likely due to a reduction in fatty acid catabolism by β-catenin–deficient osteoblasts because mice lacking carnitine palmitoyltransferase-2 in osteoblasts exhibit a similar serum lipid profile (19).

ΔCtnnb1 mice maintained normal random fed and fasting blood glucose levels (Fig. 5F), but serum insulin levels were increased in the mutants (Fig. 5G), suggesting the development of a mild insulin resistance. In accordance with this idea, the response of ΔCtnnb1 mice in glucose tolerance and insulin tolerance testing was impaired relative to littermate controls (Fig. 5H–5J), and pancreatic β-cell islets were hypertrophied (Fig. 5K and 5L). Moreover, the ability of insulin to stimulate AKT phosphorylation in gonadal adipose and the liver was reduced (Fig. 5M and 5N) and insulin responsive gene expression was altered in these tissues (Fig. 5O and 5P). In particular, the increased expression of glucose-6-phosphatase and phosphoenolpyruvate carboxykinase 1 in the liver (Fig. 5O) suggests an increase in gluconeogenesis in ΔCtnnb1 mice relative to controls. Because serum levels of undercarboxylated osteocalcin were elevated in ΔCtnnb1 mice (Fig. 5Q), presumably as a result of increased bone turnover, the most likely explanation for the impaired insulin sensitivity in the mutants is the increased uptake and deposition of lipid in liver and adipose (Fig. 4H). Thus, in addition to the development of osteopenia, the loss of β-catenin function in the mature osteoblast alters body composition as well as lipid and glucose homeostasis and thereby mirrors the effect of Lrp5 loss of function in osteoblasts on whole body metabolism (18).

Discussion

In this study, we used a series of *in vitro* and *in vivo* approaches to examine the role of β-catenin in osteoblast

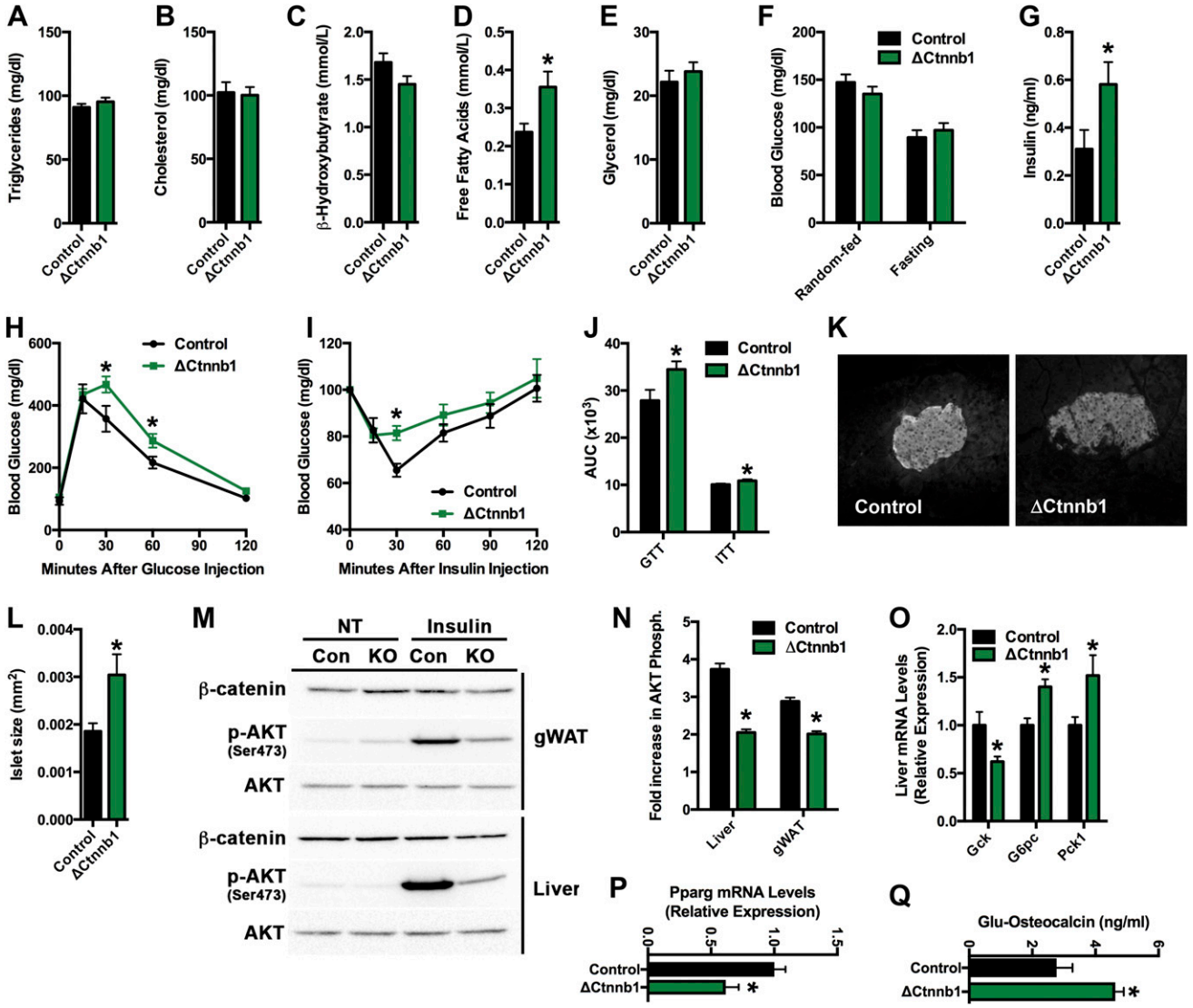

Figure 5. Fatty acid and glucose metabolism is impaired in ΔCtnnb1 mice. (A–E) Serum analysis of (A) triglycerides, (B) cholesterol, (C) β-hydroxybutyrate, (D) free fatty acids, and (E) glycerol in random-fed control and ΔCtnnb1 mice. (F) Blood glucose levels in random-fed and overnight-fasted control and ΔCtnnb1 mice. (G) Serum insulin levels in random-fed mice. (H) Glucose tolerance testing (GTT). (I) Insulin tolerance testing (ITT). (J) Area under the curve (AUC) analysis for GTT and ITT studies. (K) Representative histological images of β-cell islets immunostained for insulin (original magnification ×10). (L) Quantification of islet area. (M) Representative immunoblots of phospho-AKT (Ser473) and total AKT in gWAT and the liver of control and ΔCtnnb1 mice at baseline (NT) and after insulin administration. (N) Quantification of the fold increase in AKT phosphorylation in liver and gonadal white adipose tissue (gWAT). (O and P) qPCR analysis of insulin-responsive genes in the (O) liver and (P) gWAT of control and ΔCtnnb1 mice. (Q) Serum undercarboxylated (Glu) osteocalcin. Data are expressed as mean ± standard error of the mean; n = 5 to 10 mice per group. $^*P < 0.05$.

metabolism. Because β-catenin and Wnt signaling are essential to osteoblast maturation and function and constitutive ablation in the osteoblast lineage leads to early lethality (7, 11, 36), we produced a mouse model in which the expression of the transcription factor could be abolished postnatally *in vivo* and temporally controlled *in vitro* via the administration of TM. Our studies indicate that in addition to regulating osteoblast differentiation β-catenin is required for normal long-chain fatty acid oxidation by the osteoblast and that disrupting the expression of β-catenin in the mature osteoblast *in vivo* is sufficient to disturb lipid homeostasis and increase fat deposition.

Components of the Wnt signaling pathway have well-established roles in cellular and whole-body metabolism. As an example, polymorphisms in *LRP5* in humans are associated with obesity (37), hypertension (38), and hypercholesterolemia (39). Additionally, Tcf4 regulates metabolic activity in the liver (40), and polymorphisms in the human gene are associated with increased risk for developing type 2 diabetes (41, 42). In our previous work, the development of an increase in fat mass and dyslipidemia in mice lacking Lrp5 in the osteoblast led us to explore the connection between Wnt signaling in the skeleton and the coordination of whole-body metabolism

(18). We reported that Wnt signals emanating from Lrp5 regulate the expression of key enzymes necessary to catabolize fatty acids and that pharmacological or genetic inhibition of fatty acid oxidation in the osteoblast impairs osteoblast differentiation (18, 19).

The metabolic phenotypes of osteoblast-specific Lrp5 mutants (18) and β-catenin mutants presented here bear many similarities. Both mutants exhibited an increase in adipose tissue mass, elevated free fatty acid levels, and reduced expression of catabolic genes, which suggests that Wnt signaling regulated lipid metabolism in the osteoblast via a canonical mechanism. This idea is supported by our *in vitro* findings that revealed a reduced ability of β-catenin deficient osteoblasts to oxidize oleate, a specific effect of Wnt ligands that increase β-catenin activity on fatty acid oxidation, and our previous finding that Ctnnb1 overexpression increases oleate catabolism (18). Moreover, the fact that noncanonical Wnt ligands, such as Wnt4, Wnt5a, and Wnt5b, led to a decrease in the expression of some components (*i.e.,* Acadl) of the oxidative machinery supports this notion because noncanonical signaling has an antagonistic effect on canonical signaling (43, 44).

As with the osteoblast-specific Lrp5 mutants, we suspect that the increase in adipose tissue mass in β-catenin mutants is due to a redistribution of energy resources. Circulating free fatty acid levels were increased in β-catenin mutants, but this is unlikely to be due to an increase in lipolysis in adipocytes because the expression of genes involved in triglyceride synthesis and storage were increased in this tissue. Rather, our interpretation of the metabolic phenotype in these mice is that reduced utilization of fatty acids by the osteoblast results in a surplus of this fuel source that must be stored in other tissues. Consistent with this idea, the livers of β-catenin mutants accumulate more lipid than those of control littermates, even though markers of triglyceride synthesis are repressed and genes involved in catabolism are normal. Additionally, disrupting the expression of Cpt2, an obligate enzyme in mitochondrial long-chain fatty acid catabolism, in the osteoblast also increased serum free fatty acids levels (19). The fact that Cpt2 mutants do not also exhibit an increase in fat mass, like β-catenin and Lrp5 mutants, is due to the dramatic increase in glucose utilization in Cpt2-deficient osteoblasts that leads to a reduction in glucose storage in adipose and is able to maintain nearly normal bone volume in male mutants. Although not examined in the β-catenin mutants, high-fat diet feeding does result in a more substantial gain in adipose tissue mass in Cpt2 mutants than controls.

The development of metabolic defects in β-catenin mutants that were not evident in Lrp5 mutants, including mild steatosis, hyperinsulinemia, and reductions in glucose tolerance and insulin sensitivity, was surprising. We strongly suspect that a more severe phenotype develops in the β-catenin mutants because all effects of canonical Wnt signaling are abolished with the deletion of the pathway's target transcription factor. By comparison, Wnt signaling through the Lrp6 coreceptor will allow for some level of signaling to β-catenin to be maintained in mice in which the osteoblast is deficient for Lrp5. However, we cannot completely rule out the possibility that these disturbances are the result of defects in the second cellular pool of β-catenin that is associated with adherens junctions. It is clear that the impairments in glucose metabolism are not due to alterations in the circulating levels of hormonal osteocalcin (45), as uncarboxylated osteocalcin levels were actually increased in the mutant mice.

Intriguingly, the regulation of fatty acid oxidation by a canonical Wnt signaling mechanism involving β-catenin differs from the mechanism proposed for the utilization of glucose and glutamine after Wnt stimulation. Esen *et al.* (15) and Karner *et al.* (17) both clearly demonstrated that the utilization of these substrates in response to Wnt proceeds via the activation of mTOR signaling. This distinction could be related to changes in the preferred metabolic substrate during different stages of osteoblast maturation. Alternatively, it is possible that Wnts simultaneously regulate glucose and fatty acid utilization. The anabolic stimulus could produce an initial burst of glucose utilization via protein phosphorylation events, whereas the levels of β-catenin accumulate and then enhance the expression of genes involved in fatty acid metabolism. The observation that Wnt3a induces a rapid increase in glucose uptake and glycolysis (15) while also increasing fatty acid oxidation is compatible with this idea.

Yao and colleagues (46) also recently reported a metabolic phenotype in β-catenin mutants in which the transcription factor was targeted for postnatal recombination in osteo-progenitors via the expression of the Osx-Cre transgene (47). As in our model, the mutants developed reductions in glucose tolerance and insulin sensitivity and displayed a decrease in the mRNA levels of Cpt1b, Acadl, Acads, Acadvl, and Hadha in osteoblasts. Surprisingly, however, Yao and colleagues' (46) mutants exhibited a reduction in fat mass, opposite of what we reported here, and an increase in energy expenditure. It is possible that this phenotype is related to the fact that Osx-Cre mice exhibit a baseline phenotype that includes a reduction in body weight relative to Cre- littermates (48, 49) or the more recent observation that the Osx-Cre transgene induces recombination in tissues outside of the skeleton like the gastric and intestinal epithelium (50).

The reduction in bone volume evident in the mutant mice was expected, given the aforementioned role of β-catenin in osteoblast maturation as well as its ability

Appendix. Antibody Table

Peptide/Protein Target	Antigen Sequence (if Known)	Name of Antibody	Manufacturer, Catalog No.	Species Raised in; Monoclonal or Polyclonal	Dilution Used	RRID
Akt	—	Akt	Cell Signaling Technology, 9272	Rabbit; polyclonal	1:3000	AB_329827
Phospho-AKT	—	Phospho-Akt (Ser473)	Cell Signaling Technology, 9271	Rabbit; polyclonal	1:3000	AB_329825
Active, nonphosphorylated β-catenin	—	Nonphospho (Active) β-catenin (Ser33/37/Thr41) (D13A1)	Cell Signaling Technology, 8814	Rabbit; monoclonal	1:1000	AB_11127203
β-catenin	—	β-Catenin (D10A8)	Cell Signaling Technology, 8480	Rabbit; monoclonal	1:1000	AB_11127855
Actin	—	β-Actin (8H10D10)	Cell Signaling Technology, 3700	Mouse; monoclonal	1:10,000	AB_2242334
Insulin	—	Insulin	Dako, A056401-2	Guinea pig; polyclonal	1:1000	AB_2617169

to regulate the expression of osteoprotegerin. Serum analyses of collagen breakdown products and histomorphometric studies suggest that the loss of bone was due to a state of high bone turnover as the levels of P1NP and CTX were both increased in the serum and the numbers of both osteoblasts and osteoclasts were increased on bone surfaces. The ability of mutant osteoblasts to form a mineralized bone matrix appears to be impaired because dynamic indices of bone formation were not changed in the face of a fourfold increase in osteoblast numbers, and the expression of osteoblast markers was reduced both *in vivo* and *in vitro*. Although this was not tested directly, we predict that the increased number of osteoblasts is due to an enhancement in osteoprogenitor recruitment due to the increase in bone resorption (51) and impaired function of more differentiated osteoblasts. A similar high turnover bone loss phenotype was also reported by Chen and Long (13) when β-catenin expression was abolished postnatally in osterix-positive cells. Chen and Long's (13) β-catenin mutant also developed an increase in marrow adipocytes that was not present in our model. This is likely due to the fact that the Ocn-CreER^{T2} transgene is expressed in committed, mature osteoblasts that have lost the ability to form adipocytes, as well as the differences in the physiology of marrow adipocytes and those found in the gonadal or inguinal fat pads. As an example, marrow adipose tissue expands during caloric restriction whereas the mass of other depots declines (52–54), indicating that these cells respond differently to the metabolic cues that regulate adipocyte hypertrophy and function.

In summary, our study details the molecular mechanism by which Wnt signaling in the osteoblast directs fatty acid utilization and in turn contributes to the coordination of whole-body energy homeostasis and lipid metabolism. Distinct from the β-catenin–independent mechanism by which Wnts stimulate glucose and glutamine utilization, β-catenin accumulation and activation are required for normal lipid catabolism. These observations expand our understanding of mechanisms by which bone contributes to energy balance.

Acknowledgments

The authors thank Dr. Marie-Claude Faugere of the University of Kentucky for assistance with skeletal histomorphometric analyses.

Financial Support: This work was supported by National Institutes of Health Grants DK099134 (to R.C.R.) and NS072241 (to M.J.W.), and the John Hopkins University–University of Maryland Diabetes Research Center (Grant DK079637).

Author Contributions: R.C.R. conceived and coordinated the study and wrote the paper. J.L.F., S.P.K., Z.L., and R.C.R. designed, performed, and analyzed experiments. M.J.W. provided critical technical assistance and assisted in the preparation of the manuscript. All authors reviewed the results and approved the final version of the manuscript.

Correspondence: Ryan C. Riddle, PhD, Department of Orthopaedic Surgery, Johns Hopkins University School of Medicine, 1721 E. Madison Street, Baltimore, Maryland 21205. E-mail: rriddle1@jhmi.edu.

Disclosure Summary: The authors have nothing to disclose.

References

1. Clevers H, Nusse R. Wnt/β-catenin signaling and disease. *Cell*. 2012;**149**(6):1192–1205.
2. Boyden LM, Mao J, Belsky J, Mitzner L, Farhi A, Mitnick MA, Wu D, Insogna K, Lifton RP. High bone density due to a mutation in LDL-receptor-related protein 5. *N Engl J Med*. 2002;**346**(20):1513–1521.
3. Kato M, Patel MS, Levasseur R, Lobov I, Chang BH, Glass DA II, Hartmann C, Li L, Hwang TH, Brayton CF, Lang RA, Karsenty G, Chan L. Cbfa1-independent decrease in osteoblast proliferation, osteopenia, and persistent embryonic eye vascularization in mice deficient in Lrp5, a Wnt coreceptor. *J Cell Biol*. 2002;**157**(2):303–314.
4. Riddle RC, Diegel CR, Leslie JM, Van Koevering KK, Faugere MC, Clemens TL, Williams BO. Lrp5 and Lrp6 exert overlapping functions in osteoblasts during postnatal bone acquisition. *PLoS One*. 2013;**8**(5):e63323.
5. Gong Y, Slee RB, Fukai N, Rawadi G, Roman-Roman S, Reginato AM, Wang H, Cundy T, Glorieux FH, Lev D, Zacharin M, Oexle K,

Marcelino J, Suwairi W, Heeger S, Sabatakos G, Apte S, Adkins WN, Allgrove J, Arslan-Kirchner M, Batch JA, Beighton P, Black GC, Boles RG, Boon LM, Borrone C, Brunner HG, Carle GF, Dallapiccola B, De Paepe A, Floege B, Halfhide ML, Hall B, Hennekam RC, Hirose T, Jans A, Jüppner H, Kim CA, Keppler-Noreuil K, Kohlschuetter A, LaCombe D, Lambert M, Lemyre E, Letteboer T, Peltonen L, Ramesar RS, Romanengo M, Somer H, Steichen-Gersdorf E, Steinmann B, Sullivan B, Superti-Furga A, Swoboda W, van den Boogaard MJ, Van Hul W, Vikkula M, Votruba M, Zabel B, Garcia T, Baron R, Olsen BR, Warman ML; Osteoporosis-Pseudoglioma Syndrome Collaborative Group. LDL receptor-related protein 5 (LRP5) affects bone accrual and eye development. *Cell*. 2001;**107**(4):513–523.

6. Hill TP, Später D, Taketo MM, Birchmeier W, Hartmann C. Canonical Wnt/beta-catenin signaling prevents osteoblasts from differentiating into chondrocytes. *Dev Cell*. 2005;**8**(5):727–738.
7. Day TF, Guo X, Garrett-Beal L, Yang Y. Wnt/beta-catenin signaling in mesenchymal progenitors controls osteoblast and chondrocyte differentiation during vertebrate skeletogenesis. *Dev Cell*. 2005;**8**(5):739–750.
8. Hu H, Hilton MJ, Tu X, Yu K, Ornitz DM, Long F. Sequential roles of Hedgehog and Wnt signaling in osteoblast development. *Development*. 2005;**132**(1):49–60.
9. Tan SH, Senarath-Yapa K, Chung MT, Longaker MT, Wu JY, Nusse R. Wnts produced by Osterix-expressing osteolineage cells regulate their proliferation and differentiation. *Proc Natl Acad Sci USA*. 2014;**111**(49):E5262–E5271.
10. Bao Q, Chen S, Qin H, Feng J, Liu H, Liu D, Li A, Shen Y, Zhong X, Li J, Zong Z. Constitutive β-catenin activation in osteoblasts impairs terminal osteoblast differentiation and bone quality. *Exp Cell Res*. 2017;**350**(1):123–131.
11. Holmen SL, Zylstra CR, Mukherjee A, Sigler RE, Faugere MC, Bouxsein ML, Deng L, Clemens TL, Williams BO. Essential role of beta-catenin in postnatal bone acquisition. *J Biol Chem*. 2005;**280**(22):21162–21168.
12. Cawthorn WP, Bree AJ, Yao Y, Du B, Hemati N, Martinez-Santibañez G, MacDougald OA. Wnt6, Wnt10a and Wnt10b inhibit adipogenesis and stimulate osteoblastogenesis through a β-catenin-dependent mechanism. *Bone*. 2012;**50**(2):477–489.
13. Chen J, Long F. β-catenin promotes bone formation and suppresses bone resorption in postnatal growing mice. *J Bone Miner Res*. 2013;**28**(5):1160–1169.
14. Glass II DA, Bialek P, Ahn JD, Starbuck M, Patel MS, Clevers H, Taketo MM, Long F, McMahon AP, Lang RA, Karsenty G. Canonical Wnt signaling in differentiated osteoblasts controls osteoclast differentiation. *Dev Cell*. 2005;**8**(5):751–764.
15. Esen E, Chen J, Karner CM, Okunade AL, Patterson BW, Long F. WNT-LRP5 signaling induces Warburg effect through mTORC2 activation during osteoblast differentiation. *Cell Metab*. 2013;**17**(5):745–755.
16. Otsuka E, Yamaguchi A, Hirose S, Hagiwara H. Characterization of osteoblastic differentiation of stromal cell line ST2 that is induced by ascorbic acid. *Am J Physiol*. 1999;**277**(1 Pt 1):C132–C138.
17. Karner CM, Esen E, Okunade AL, Patterson BW, Long F. Increased glutamine catabolism mediates bone anabolism in response to WNT signaling. *J Clin Invest*. 2015;**125**(2):551–562.
18. Frey JL, Li Z, Ellis JM, Zhang Q, Farber CR, Aja S, Wolfgang MJ, Clemens TL, Riddle RC. Wnt-Lrp5 signaling regulates fatty acid metabolism in the osteoblast. *Mol Cell Biol*. 2015;**35**(11):1979–1991.
19. Kim SP, Li Z, Zoch ML, Frey JL, Bowman CE, Kushwaha P, Ryan KA, Goh BC, Scafidi S, Pickett JE, Faugere MC, Kershaw EE, Thorek DLJ, Clemens TL, Wolfgang MJ, Riddle RC. Fatty acid oxidation by the osteoblast is required for normal bone acquisition in a sex- and diet-dependent manner. *JCI Insight*. 2017;**2**(16):2.
20. Brault V, Moore R, Kutsch S, Ishibashi M, Rowitch DH, McMahon AP, Sommer L, Boussadia O, Kemler R. Inactivation of the beta-catenin gene by Wnt1-Cre-mediated deletion results in dramatic brain malformation and failure of craniofacial development. *Development*. 2001;**128**(8):1253–1264.
21. Yoshikawa Y, Kode A, Xu L, Mosialou I, Silva BC, Ferron M, Clemens TL, Economides AN, Kousteni S. Genetic evidence points to an osteocalcin-independent influence of osteoblasts on energy metabolism. *J Bone Miner Res*. 2011;**26**(9):2012–2025.
22. Ellis JM, Wong GW, Wolfgang MJ. Acyl coenzyme A thioesterase 7 regulates neuronal fatty acid metabolism to prevent neurotoxicity. *Mol Cell Biol*. 2013;**33**(9):1869–1882.
23. Li Z, Frey JL, Wong GW, Faugere MC, Wolfgang MJ, Kim JK, Riddle RC, Clemens TL. Glucose Transporter-4 Facilitates Insulin-Stimulated Glucose Uptake in Osteoblasts. *Endocrinology*. 2016;**157**(11):4094–4103.
24. Bouxsein ML, Boyd SK, Christiansen BA, Guldberg RE, Jepsen KJ, Müller R. Guidelines for assessment of bone microstructure in rodents using micro-computed tomography. *J Bone Miner Res*. 2010;**25**(7):1468–1486.
25. Parfitt AM, Drezner MK, Glorieux FH, Kanis JA, Malluche H, Meunier PJ, Ott SM, Recker RR. Bone histomorphometry: standardization of nomenclature, symbols, and units. Report of the ASBMR Histomorphometry Nomenclature Committee. *J Bone Miner Res*. 1987;**2**(6):595–610.
26. Dempster DW, Compston JE, Drezner MK, Glorieux FH, Kanis JA, Malluche H, Meunier PJ, Ott SM, Recker RR, Parfitt AM. Standardized nomenclature, symbols, and units for bone histomorphometry: a 2012 update of the report of the ASBMR Histomorphometry Nomenclature Committee. *J Bone Miner Res*. 2013;**28**(1):2–17.
27. Xiao F, Huang Z, Li H, Yu J, Wang C, Chen S, Meng Q, Cheng Y, Gao X, Li J, Liu Y, Guo F. Leucine deprivation increases hepatic insulin sensitivity via GCN2/mTOR/S6K1 and AMPK pathways. *Diabetes*. 2011;**60**(3):746–756.
28. Zhang Q, Yu J, Liu B, Lv Z, Xia T, Xiao F, Chen S, Guo F. Central activating transcription factor 4 (ATF4) regulates hepatic insulin resistance in mice via S6K1 signaling and the vagus nerve. *Diabetes*. 2013;**62**(7):2230–2239.
29. Hussain MA, Porras DL, Rowe MH, West JR, Song WJ, Schreiber WE, Wondisford FE. Increased pancreatic beta-cell proliferation mediated by CREB binding protein gene activation. *Mol Cell Biol*. 2006;**26**(20):7747–7759.
30. Andrade AC, Nilsson O, Barnes KM, Baron J. Wnt gene expression in the post-natal growth plate: regulation with chondrocyte differentiation. *Bone*. 2007;**40**(5):1361–1369.
31. Ayturk UM, Jacobsen CM, Christodoulou DC, Gorham J, Seidman JG, Seidman CE, Robling AG, Warman ML. An RNA-seq protocol to identify mRNA expression changes in mouse diaphyseal bone: applications in mice with bone property altering Lrp5 mutations. *J Bone Miner Res*. 2013;**28**(10):2081–2093.
32. Jho EH, Zhang T, Domon C, Joo CK, Freund JN, Costantini F. Wnt/beta-catenin/Tcf signaling induces the transcription of Axin2, a negative regulator of the signaling pathway. *Mol Cell Biol*. 2002;**22**(4):1172–1183.
33. Leung JY, Kolligs FT, Wu R, Zhai Y, Kuick R, Hanash S, Cho KR, Fearon ER. Activation of AXIN2 expression by beta-catenin-T cell factor. A feedback repressor pathway regulating Wnt signaling. *J Biol Chem*. 2002;**277**(24):21657–21665.
34. Liu J, Wu X, Mitchell B, Kintner C, Ding S, Schultz PG. A small-molecule agonist of the Wnt signaling pathway. *Angew Chem Int Ed Engl*. 2005;**44**(13):1987–1990.
35. Gwak J, Hwang SG, Park HS, Choi SR, Park SH, Kim H, Ha NC, Bae SJ, Han JK, Kim DE, Cho JW, Oh S. Small molecule-based disruption of the Axin/β-catenin protein complex regulates mesenchymal stem cell differentiation. *Cell Res*. 2012;**22**(1):237–247.
36. Kramer I, Halleux C, Keller H, Pegurri M, Gooi JH, Weber PB, Feng JQ, Bonewald LF, Kneissel M. Osteocyte Wnt/beta-catenin signaling is required for normal bone homeostasis. *Mol Cell Biol*. 2010;**30**(12):3071–3085.

37. Guo YF, Xiong DH, Shen H, Zhao LJ, Xiao P, Guo Y, Wang W, Yang TL, Recker RR, Deng HW. Polymorphisms of the low-density lipoprotein receptor-related protein 5 (LRP5) gene are associated with obesity phenotypes in a large family-based association study. *J Med Genet*. 2006;**43**(10):798–803.
38. Suwazono Y, Kobayashi E, Uetani M, Miura K, Morikawa Y, Ishizaki M, Kido T, Nakagawa H, Nogawa K. Low-density lipoprotein receptor-related protein 5 variant Q89R is associated with hypertension in Japanese females. *Blood Press*. 2006;**15**(2):80–87.
39. Suwazono Y, Kobayashi E, Uetani M, Miura K, Morikawa Y, Ishizaki M, Kido T, Nakagawa H, Nogawa K. G-protein beta 3 subunit polymorphism C1429T and low-density lipoprotein receptor-related protein 5 polymorphism A1330V are risk factors for hypercholesterolemia in Japanese males–a prospective study over 5 years. *Metabolism*. 2006;**55**(6):751–757.
40. Boj SF, van Es JH, Huch M, Li VS, José A, Hatzis P, Mokry M, Haegebarth A, van den Born M, Chambon P, Voshol P, Dor Y, Cuppen E, Fillat C, Clevers H. Diabetes risk gene and Wnt effector Tcf7l2/TCF4 controls hepatic response to perinatal and adult metabolic demand. *Cell*. 2012;**151**(7):1595–1607.
41. Grant SF, Thorleifsson G, Reynisdottir I, Benediktsson R, Manolescu A, Sainz J, Helgason A, Stefansson H, Emilsson V, Helgadottir A, Styrkarsdottir U, Magnusson KP, Walters GB, Palsdottir E, Jonsdottir T, Gudmundsdottir T, Gylfason A, Saemundsdottir J, Wilensky RL, Reilly MP, Rader DJ, Bagger Y, Christiansen C, Gudnason V, Sigurdsson G, Thorsteinsdottir U, Gulcher JR, Kong A, Stefansson K. Variant of transcription factor 7-like 2 (TCF7L2) gene confers risk of type 2 diabetes. *Nat Genet*. 2006;**38**(3):320–323.
42. Tong Y, Lin Y, Zhang Y, Yang J, Zhang Y, Liu H, Zhang B. Association between TCF7L2 gene polymorphisms and susceptibility to type 2 diabetes mellitus: a large Human Genome Epidemiology (HuGE) review and meta-analysis. *BMC Med Genet*. 2009;**10**(1):15.
43. Stoick-Cooper CL, Weidinger G, Riehle KJ, Hubbert C, Major MB, Fausto N, Moon RT. Distinct Wnt signaling pathways have opposing roles in appendage regeneration. *Development*. 2007; **134**(3):479–489.
44. Topol L, Jiang X, Choi H, Garrett-Beal L, Carolan PJ, Yang Y. Wnt-5a inhibits the canonical Wnt pathway by promoting GSK-3-independent beta-catenin degradation. *J Cell Biol*. 2003;**162**(5): 899–908.
45. Lee NK, Sowa H, Hinoi E, Ferron M, Ahn JD, Confavreux C, Dacquin R, Mee PJ, McKee MD, Jung DY, Zhang Z, Kim JK, Mauvais-Jarvis F, Ducy P, Karsenty G. Endocrine regulation of energy metabolism by the skeleton. *Cell*. 2007;**130**(3):456–469.
46. Yao Q, Yu C, Zhang X, Zhang K, Guo J, Song L. Wnt/β-catenin signaling in osteoblasts regulates global energy metabolism. *Bone*. 2017;**97**:175–183.
47. Rodda SJ, McMahon AP. Distinct roles for Hedgehog and canonical Wnt signaling in specification, differentiation and maintenance of osteoblast progenitors. *Development*. 2006;**133**(16): 3231–3244.
48. Davey RA, Clarke MV, Sastra S, Skinner JP, Chiang C, Anderson PH, Zajac JD. Decreased body weight in young Osterix-Cre transgenic mice results in delayed cortical bone expansion and accrual. *Transgenic Res*. 2012;**21**(4):885–893.
49. Huang W, Olsen BR. Skeletal defects in Osterix-Cre transgenic mice. *Transgenic Res*. 2015;**24**(1):167–172.
50. Chen J, Shi Y, Regan J, Karuppaiah K, Ornitz DM, Long F. Osx-Cre targets multiple cell types besides osteoblast lineage in postnatal mice. *PLoS One*. 2014;**9**(1):e85161.
51. Tang Y, Wu X, Lei W, Pang L, Wan C, Shi Z, Zhao L, Nagy TR, Peng X, Hu J, Feng X, Van Hul W, Wan M, Cao X. TGF-beta1-induced migration of bone mesenchymal stem cells couples bone resorption with formation. *Nat Med*. 2009;**15**(7):757–765.
52. Cawthorn WP, Scheller EL, Parlee SD, Pham HA, Learman BS, Redshaw CM, Sulston RJ, Burr AA, Das AK, Simon BR, Mori H, Bree AJ, Schell B, Krishnan V, MacDougald OA. Expansion of Bone Marrow Adipose Tissue During Caloric Restriction Is Associated With Increased Circulating Glucocorticoids and Not With Hypoleptinemia. *Endocrinology*. 2016;**157**(2):508–521.
53. Devlin MJ, Cloutier AM, Thomas NA, Panus DA, Lotinun S, Pinz I, Baron R, Rosen CJ, Bouxsein ML. Caloric restriction leads to high marrow adiposity and low bone mass in growing mice. *J Bone Miner Res*. 2010;**25**(9):2078–2088.
54. Bredella MA, Fazeli PK, Miller KK, Misra M, Torriani M, Thomas BJ, Ghomi RH, Rosen CJ, Klibanski A. Increased bone marrow fat in anorexia nervosa. *J Clin Endocrinol Metab*. 2009; **94**(6):2129–2136.